



Power Loss Analysis in a SiC/IGBT Propulsion Inverter Including Blanking Time, MOSFET's Reverse Conduction and the Effect of Thermal Feedback

Downloaded from: <https://research.chalmers.se>, 2025-05-23 22:03 UTC

Citation for the original published paper (version of record):

Amirpour, S., Thiringer, T., Hagstedt, D. (2020). Power Loss Analysis in a SiC/IGBT Propulsion Inverter Including Blanking Time, MOSFET's Reverse Conduction and the Effect of Thermal Feedback Using a PMSM Model. IECON Proceedings (Industrial Electronics Conference)(2020): 1424-1430.
<http://dx.doi.org/10.1109/IECON43393.2020.9254297>

N.B. When citing this work, cite the original published paper.

© 2020 IEEE. Personal use of this material is permitted. Permission from IEEE must be obtained for all other uses, in any current or future media, including reprinting/republishing this material for advertising or promotional purposes, or reuse of any copyrighted component of this work in other works.

Power Loss Analysis in a SiC/IGBT Propulsion Inverter Including Blanking Time, MOSFET's Reverse Conduction and the Effect of Thermal Feedback Using a PMSM Model

Sepideh Amirpour
Department of Powertrain Engineering
China Euro Vehicle Technology AB
Gothenburg, Sweden
sepideh.amirpour@cevt.se

Torbjörn Thiringer
Department of Electrical Engineering
Chalmers University of Technology
Gothenburg, Sweden
torbjorn.thiringer@chalmers.se

Dan Hagstedt
Department of Powertrain Engineering
China Euro Vehicle Technology AB
Gothenburg, Sweden
Dan.Hagstedt@cevt.se

Abstract— This paper presents a comparison of power losses for two silicon carbide (SiC) and one silicon insulated gate bipolar transistor (Si IGBT) power modules in a three-phase inverter, when considering the effect of blanking time and the MOSFET's reverse conduction. The total power losses versus different switching frequencies are also compared for the three inverters. The focus of this paper is to determine the influence of junction temperature and thermal feedback on the power loss calculation. The analysis shows that, without accounting for the thermal feedback, the loss levels are substantially underestimated, 11-15% on the conduction losses of the SiC inverters and up to 18% on the switching losses of the IGBT inverter. The data is derived at a chosen high torque, low speed operating point of a permanent magnet synchronous machine (PMSM). The operating point is considered as a worse operating condition from the power loss perspective.

Keywords— Silicon Carbide (SiC), Voltage Source Inverters (VSI), MOSFET Reverse Conduction, Thermal Feedback, Electric Vehicle

I. INTRODUCTION

The demand for reduced power and energy losses in propulsion inverters especially for electric drive (EV) and hybrid powertrains is continuously increasing [1]. New generations of commercial Wide Band Gap silicon carbide (SiC) MOSFETs seem to be a promising alternative compared to commonly used silicon insulated gate bipolar transistors (Si IGBTs) in electrified vehicle applications [2],[3]. Lower switching losses due to faster switching transitions, combined with better thermal properties make these an attractive option to Si IGBTs. In addition, lower conduction losses can be achieved by the MOSFET's reverse conduction phenomenon. By improving the efficiency of the propulsion inverter, the overall efficiency of the powertrain can be improved, which results in a lighter cooling system, higher power density, increased range, etc. Several research works have been presented, where SiC MOSFETs and traditional Si IGBTs are compared for EV-applications with respect to energy efficiency [2], [3], along with taking temperature effect into account by ANSYS finite element analysis (FEM) in [4] and the MOSFET's reverse conduction when an electro-thermal calculation is considered for the comparisons in [5]. However, there is a lack of comprehensive comparisons which numerically quantifies the effect of considering and neglecting the thermal feedback on the power loss calculations for the

operating regions of a permanent magnet synchronous machine (PMSM) while covering the impacts of blanking time and MOSFET's reverse conduction.

The purpose of this paper is to compare the power losses with and without the effect of the thermal feedback of a recently introduced 3rd generation half-bridge SiC module, CAB450M12XM3 and the 2nd generation, CAS300M12BM2 in the 1200V class with a 1200V Si IGBT, FZ600R12KE3 for the relevant operating points of a PMSM. The blanking time as well as the MOSFET's reverse conduction are taken into account. The total losses of the propulsion inverter for the three modules are derived by implementing space vector modulation (SVM) and making a comparison for the whole operating regions of a PMSM. In Fig. 1, an overview of the analysis is illustrated.

II. REVERSE CONDUCTION AND BLANKING TIME

A major difference of the investigated modules is their current conduction behavior. In Si IGBTs the total reverse current of the transistor flows through an anti-parallel diode, while MOSFETs through their reverse conduction characteristic can also conduct in the opposite direction. In the inverter, either the upper or the lower diode in one leg is conducting when the current and voltage have different signs in the same phase leg. Therefore, if the corresponding MOSFET's drain to source voltage gets higher than the diode's threshold voltage, parallel conduction of the two devices occurs. The diode can either be a separate diode or the intrinsic inbuilt one. This capability influences the conduction losses distribution in SiC MOSFET modules, resulting in reduced power losses.

To avoid a shoot through fault in a pulse width modulation (PWM) controlled inverter, a blanking time is

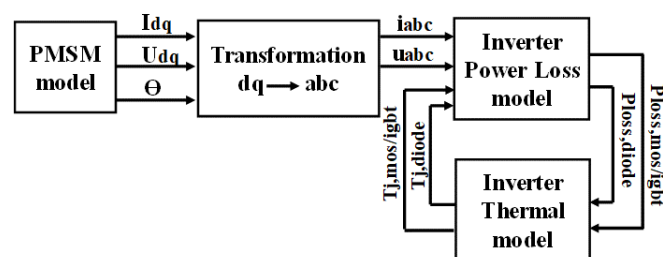


Fig. 1. System simulation model overview.

introduced, where both the upper and lower switches in the same phase leg are off and only the diode is conducting during this time. In this way, the risk of a short circuit of the dc-link can be reduced. However, the total conduction loss of the modules is influenced by the diode conduction during the blanking time.

III. CONDUCTION LOSSES INCLUDING BLANKING TIME AND MOSFET'S REVERSE CONDUCTION

A. Conduction Losses in the SiC Power Module

In this study, the conduction losses for a three-phase voltage source inverter are determined numerically using MATLAB. The used numerical implementation is based on an analytical approach for SiC MOSFETs' conduction losses which is presented in [5], [6]. In this approach, the average MOSFET conduction losses over a fundamental period of the phase current can be calculated as

$$P_{cond,MOS} = \frac{1}{2\pi} \int_0^{2\pi} R_{on} I_M^2(\alpha) \tau(\alpha) d\alpha \quad (1)$$

where R_{on} is the MOSFET on-state resistance, I_M is the MOSFET current, $\alpha = 2\pi ft$ where f is the fundamental frequency and τ is the duty cycle which can be expressed as a function of α as

$$\tau(\alpha) = \frac{1}{2} (1 + m \sin \alpha) \quad (2)$$

where m is the modulation index [7]. Likewise, the diode conduction losses can be derived as

$$P_{cond,D} = \frac{1}{2\pi} \int_0^{2\pi} (R_d I_D^2(\alpha) + V_d I_D(\alpha)) \tau(\alpha) d\alpha \quad (3)$$

where the voltage drop, V_d , and the on-state resistance, R_d , can be obtained from the datasheet information of the forward characteristics of the diode, I_D is the diode current.

During reverse conduction, the MOSFET and diode's current can be obtained as

$$I_M = \frac{R_d I_p \sin(\alpha - \varphi) - V_d}{R_d + R_{on}} \quad (4)$$

$$I_D = \frac{R_{on} I_p \sin(\alpha - \varphi) + V_d}{R_d + R_{on}} \quad (5)$$

where φ is the angle of displacement power factor and I_p is the peak phase current [6].

In Fig. 2 the losses with and without MOSFET reverse conduction are presented for the upper diode and MOSFET in a phase leg of CAS300, SiC inverter. A significant reduction in diodes' total conduction losses up to 83% as the result of parallel conduction is observed. The operating condition used for calculating the losses are presented in Table I. Likewise, for CAB450 inverter, a reduction up to 97% in diodes' conduction losses is noticed.

B. Conduction Losses in the IGBT Power Module

The conduction losses of a Si IGBT and diode in a Si IGBT module can be calculated by integrating the product of the current flowing through the device and voltage drop over it [8], [9], resulting in the expressions as

$$P_{cond,IGBT} = \frac{1}{2} \left(V_T \frac{I_p}{\pi} + R_f \frac{I_p^2}{4} \right) + m \cos \varphi \left(V_T \frac{I_p}{8} + \frac{1}{3\pi} R_f I_p^2 \right) \quad (6)$$

$$P_{cond,Diode} = \frac{1}{2} \left(V_d \frac{I_p}{\pi} + R_d \frac{I_p^2}{4} \right) - m \cos \varphi \left(V_d \frac{I_p}{8} + \frac{1}{3\pi} R_d I_p^2 \right) \quad (7)$$

where R_f is the IGBT on-state resistance and V_T is the IGBT voltage drop.

C. Blanking Time

In order to include the effect of the blanking time in the conduction power losses calculation, an equivalent duty cycle to be used in the above-mentioned conduction loss equations, can be introduced as

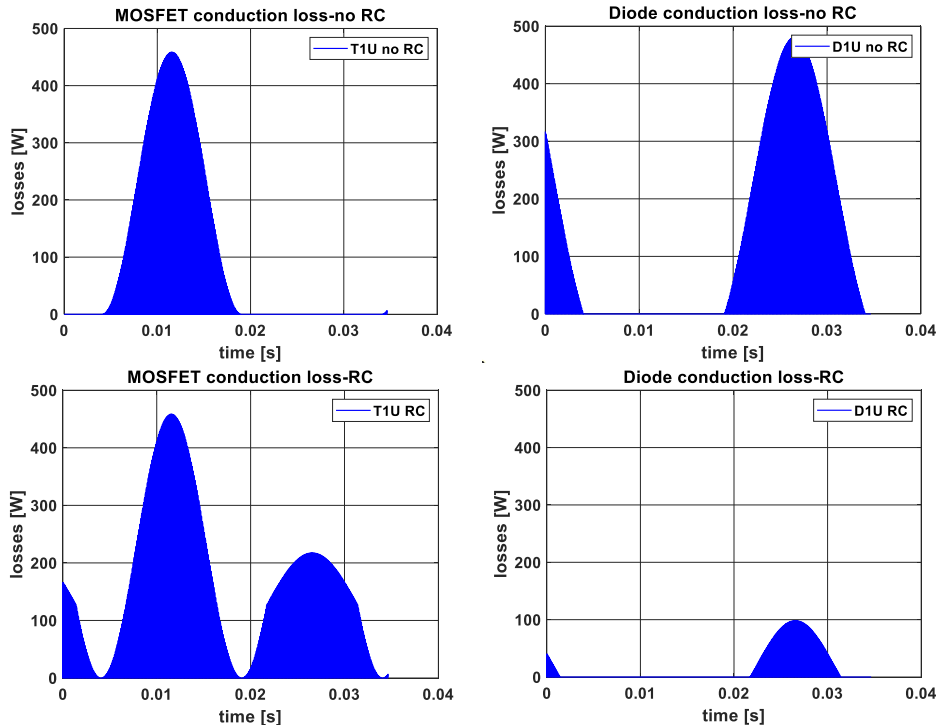


Fig. 2. MOSFET and Diode conduction losses with and without MOSFET reverse conduction (RC) in CAS300, SiC inverter, upper MOSFET and Diode in a phase leg.

TABLE I. CHOSEN OPERATING POINT OF PMSM FOR THE THREE INVERTERS POWER LOSS COMPARISON

Variable	Value	Unit
Current magnitude	565	[A]
DC voltage	300	[V]
Blanking time	0.5	[μ s]
Switching Frequency	10	[kHz]
Modulation index	0.084	[-]
Torque	160	[Nm]
Mechanical speed	500	[rpm]

$$\tau_{eq}(\alpha) = \tau(\alpha) - t_{blanking}f_{sw} = \frac{1}{2}(1 - 2t_{blanking}f_{sw} + msina) \quad (8)$$

where f_{sw} is the switching frequency [6].

Fig. 3 shows the diode and MOSFET currents in a phase leg of the CAS300 inverter, without (upper one) and with (lower one) the effect of blanking time, when also considering the MOSFET reverse conduction. As shown in the lower figure, during the blanking time, only the diode is conducting the current. This leads to an increase of 20 W (12%) on the diodes' conduction losses for CAS300 inverter, when considering the MOSFET reverse conduction. The effect on the MOSFETs' conduction losses is small and not considerable. For CAB450 and FZ600, an increase up to 70 W and 10 W, on the diodes' conduction losses is observed, respectively. Fig.4 illustrates the upper diode conduction losses in a phase leg of CAS300, without and with blanking time, when the MOSFET reverse conduction is also considered. The operating condition used for calculating the diodes' conduction losses, is given in Table I.

IV. SWITCHING LOSSES IN IGBT AND SIC MOSFET

During every turn on and turn off event, a loss occurs in the switch and its anti-parallel/body-diode. The switching energy of the Si IGBTs and diodes are generally higher than those of the SiC devices. Switching losses can be calculated in an IGBT, MOSFET and diode analytically by the expression as

$$P_{sw.MOSFET,IGBT,Diode} = f_{sw} \cdot E_{sw}(@I_{nom},V_{nom}) \cdot \left(\frac{1}{\pi} \frac{I_p}{I_{nom}}\right)^{k_i} \cdot \left(\frac{V_{dc}}{V_{nom}}\right)^{k_v} \quad (9)$$

where E_{sw} is switching energy loss, I_p is the peak phase current, I_{nom} and V_{nom} are nominal current and voltage values and k_i , k_v are current and voltage dependency exponents, respectively [9]. In the numerical implementation in this study, the switching loss is calculated at every switch-on and switch-off event of the device as

$$P_{sw} = \frac{\sum E_{sw}}{t} \quad (10)$$

where t is the total simulation time.

V. THERMAL CALCULATION MODEL

As some parameters in the power modules, such as on-state resistances, forward voltage drops, switching and reverse recovery energies are temperature-dependent, the inverters' power losses are found by using a thermal network which is presented in Fig. 5 for the compared modules. T_j , represents the junction temperatures of MOSFET/IGBTs and diodes, T_c is the case temperature, T_s and T_f represent the heatsink and

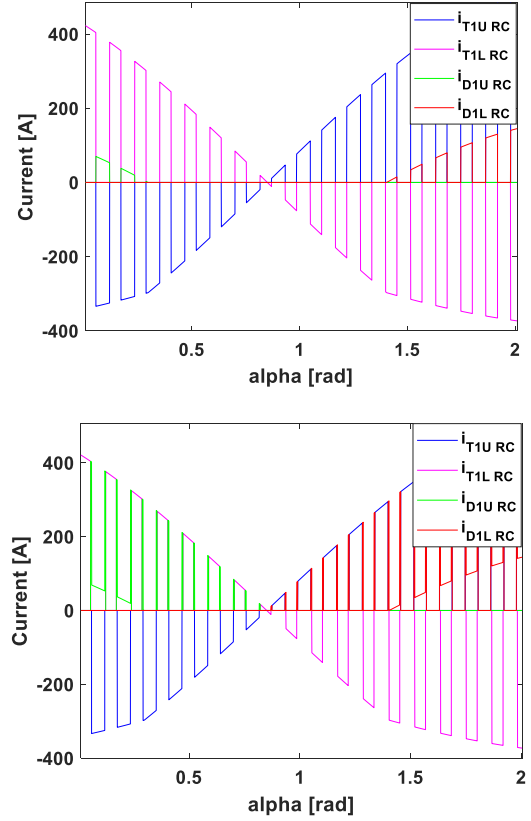


Fig. 3. Impact of blanking time on diode and MOSFET currents as function of $\alpha = 2\pi ft$ with considering the MOSFET's reverse conduction in a phase leg of CAS300 inverter. Upper figure with no blanking time, lower figure with blanking time.

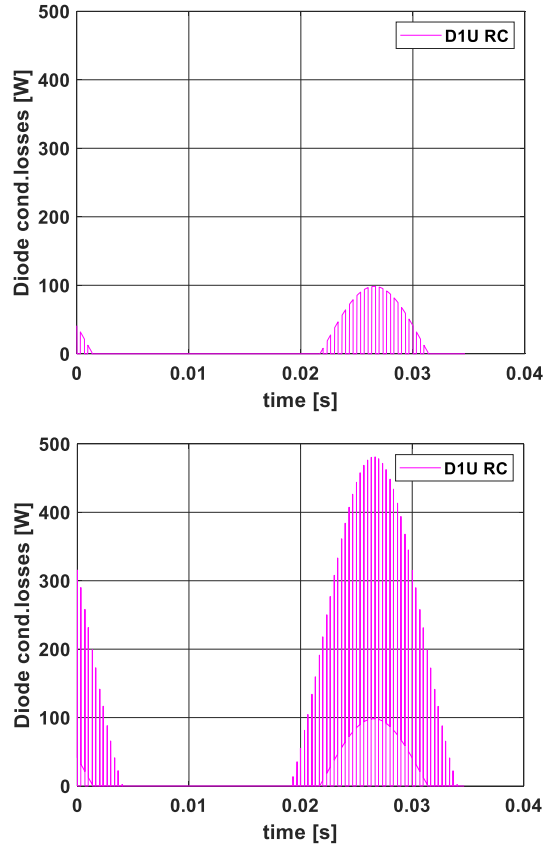


Fig. 4. Diode conduction loss, no blanking time (top), with blanking time (bottom) in a phase leg of CAS300 inverter.

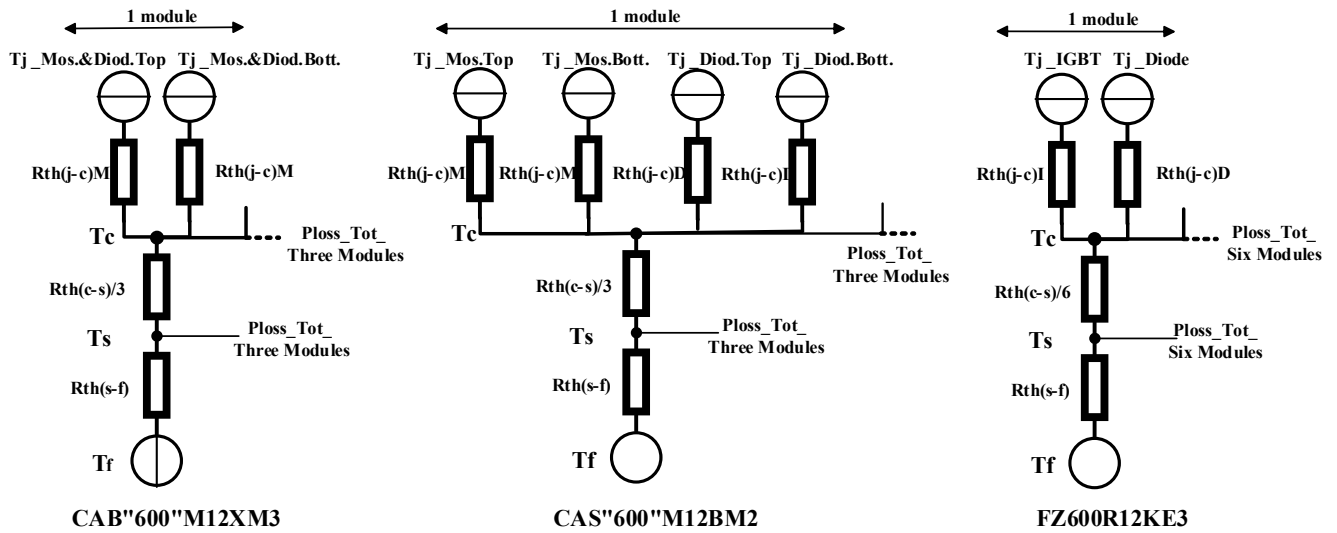


Fig. 5. Thermal calculation model to find the power losses and temperatures.

fluid temperatures, respectively. For a fair comparison, the same heatsink is used for each inverter although it would have been possible to use a smaller one for the SiC MOSFET inverters. Worth mentioning is that, for the SiC-based inverters, three SiC half-bridge modules are used and for the IGBT-based inverter, six IGBT modules are used. All set-ups are normalized to the same current rating level of 600 A. The fluid temperature and fluid flow rate are set to 65 °C and 10 L/min, respectively. It can be noted that, the CAB450 module is using the latest 3rd GEN MOSFET dies which have an inbuilt body diode, hence the module does not have an antiparallel diode, as can be seen in Fig. 5, compared to CAS300 which has an additional antiparallel Schottky diode with zero reverse recovery energy.

VI. COMPARISON OF LOSSES IN THREE PHASE SiC/IGBT INVERTERS WITH AND WITHOUT THERMAL FEEDBACK

To compare the power losses of the three investigated modules, an operating point of a PMSM at high torque, high current magnitude and low speed is used. The chosen operating point can be considered as a worse operating condition in the urban driving cycles from the power loss point of view. The PMSM is controlled by implementing a control

TABLE II. PMSM RATING PARAMETERS

Variable	Value	Unit
DC-Link voltage	300	[V]
Rated current	400 RMS	[A]
Pole Pairs	4	[-]
Maximum speed	12000	[rpm]
Maximum torque	160	[Nm]

strategy comprising of Maximum Torque per Ampere (MTPA) and Maximum Torque per Volt (MTPV) control. Under this control strategy, the PMSM operates in constant torque range as well as in the partial and full field weakening ranges [10], [11]. The chosen operating point is shown in Table I and the rating parameters of the PMSM are given in Table II. The losses are calculated based on the temperature through an iterative approach in which, the devices' static and dynamic parameters (V_T , V_d , R_f , R_d , R_{on} , E_{sw} and E_{rr}) are interpolated based on the junction temperature, then the losses and the temperatures are redetermined sequentially and iteratively until convergence. It can be noted that, the current dependency of the devices' switching energies is considered by interpolating the switching energies as function of current

TABLE III. SIMULATED AVERAGE VALUE OF CONDUCTION AND SWITCHING LOSSES OF THE SiC INVERTER WITH AND WITHOUT THERMAL FEEDBACK, CONSIDERING BLANKING TIME AND USING THE MOSFET'S REVERSE CONDUCTION AT 160 NM, 500 RPM MECHANICAL SPEED AND $T_f = 65^\circ\text{C}$.

CAB "600" M12XM3									
	Cond. [W]	Cond. Thermal Feedback [W]	Diff. [W]	Diff.%	Sw. [W]	Sw. Thermal Feedback [W]	Diff. [W]	Diff.%	Tjunc. Thermal Feedback [°C]
MOSFETs	977.8	1140.5	162.7	16.6	206.6	206.8	0.2	0.09	99.8
Diodes	74.4	72.4	-2	-2.7	3.51	3.52	0.01	0.28	99.8
Tot. Inverter	1052.2	1212.9	160.7	15.3	210.1	210.3	0.22	0.1	
CAS "600" M12BM2									
	Cond. [W]	Cond. Thermal Feedback [W]	Diff. [W]	Diff.%	Sw. [W]	Sw. Thermal Feedback [W]	Diff. [W]	Diff.%	Tjunc. Thermal Feedback [°C]
MOSFETs	1072	1164	92	8.6	196.3	196.5	0.2	0.1	95.6
Diodes	140.1	182.1	42	29.9	0	0	0	0	88.2
Tot. Inverter	1212.1	1346.1	134	11	196.3	196.5	0.2	0.1	

TABLE IV. SIMULATED AVERAGE VALUE OF CONDUCTION AND SWITCHING LOSSES OF THE IGBT INVERTER WITH AND WITHOUT THERMAL FEEDBACK, CONSIDERING BLANKING TIME AT 160 NM, 500 RPM MECHANICAL SPEED AND $T_f = 65^\circ\text{C}$.

FZ600R12KE3									
	Cond. [W]	Cond. Thermal Feedback [W]	Diff. [W]	Diff. %	Sw. [W]	Sw. Thermal Feedback [W]	Diff. [W]	Diff. %	Tjunc. Thermal Feedback $^\circ\text{C}$
IGBTs	738.0	774.7	36.7	5	713.7	807.8	94.1	13.1	95.6
Diodes	809.9	793.2	-16.7	-2	426.7	532.1	105.4	24.7	103.3
Tot. Inverter	1547.9	1567.9	20	1.3	1140.4	1339.9	199.5	17.5	

as well as the junction temperature. The results of the investigations are presented in Tables III and IV for SiC modules and Si IGBT, respectively. Worth mentioning is that, in order to have the same nominal current of 600 A for the three compared modules, a scale factor is applied on the power losses of the SiC modules for a fair comparison.

According to the simulated values shown in Tables III and IV, a significant decrease in diode conduction losses can be observed for the two SiC modules compared to the Si IGBT module. This can be explained as a result of the MOSFET's reverse conduction capability where the current between the diode and the MOSFET is shared. Moreover, from thermal point of view, for the SiC MOSFETs, the rate of increase of the conduction losses with respect to junction temperature is relatively high when compared to that of a Si IGBT. The reason is a lower increase in the IGBT dynamic on-state resistance with an increase of junction temperature. However, higher switching losses in the Si IGBT is observed substantially, which is limiting its usability for high frequency applications. In addition, the increment of IGBT switching losses with respect to an increase in temperature is relatively high compared to its conduction losses. In SiC-MOSFETs, the effect of a temperature increase on the switching losses is almost zero.

A comparison between the two SiC modules shows a considerable reduction in conduction losses especially in the CAB“600” diodes, since it is using the latest 3rd GEN MOSFET dies with a very robust intrinsic body diode and can operate reliably in the 3rd quadrant, compared to CAS“600”

with external anti-parallel diodes. In the SiC modules, the increase rate of conduction losses in the diodes (body diode or possible external diode) with respect to an increase in junction temperature is much lower compared to that in the channel of MOSFETs. This is due to a lower increase in the diode dynamic resistance with temperature.

All in all, at the chosen operating point, despite the higher conduction losses in MOSFETs, compared to that of IGBTs, the total losses in the SiC inverters is considerably lower. This is due to the fact that, the switching losses in IGBTs and diodes in FZ600 inverter as well as the conduction losses in the diodes of FZ600 are higher compared to those of the SiC inverters. The total conduction and switching losses of the FZ600 inverter with the thermal feedback are 2908 W which means that, 1485 W and 1365 W higher than that of the CAB“600” and CAS“600” inverters, respectively. Moreover, the impact of the thermal feedback on the inverters' total losses is, an increase up to 11-15% and 18% at the chosen operating condition for the SiCs' conduction losses and IGBTs' switching losses, respectively.

VII. INVERTERS' TOTAL POWER LOSSES WITH THERMAL FEEDBACK AND LOSS DIFFERENCES WITHOUT THERMAL FEEDBACK

In Figs. 6 and 7, the total power losses of the three-phase propulsion inverter for the three compared modules are presented as function of torque and rotational speed. The data is derived before and after the thermal feedback is applied to

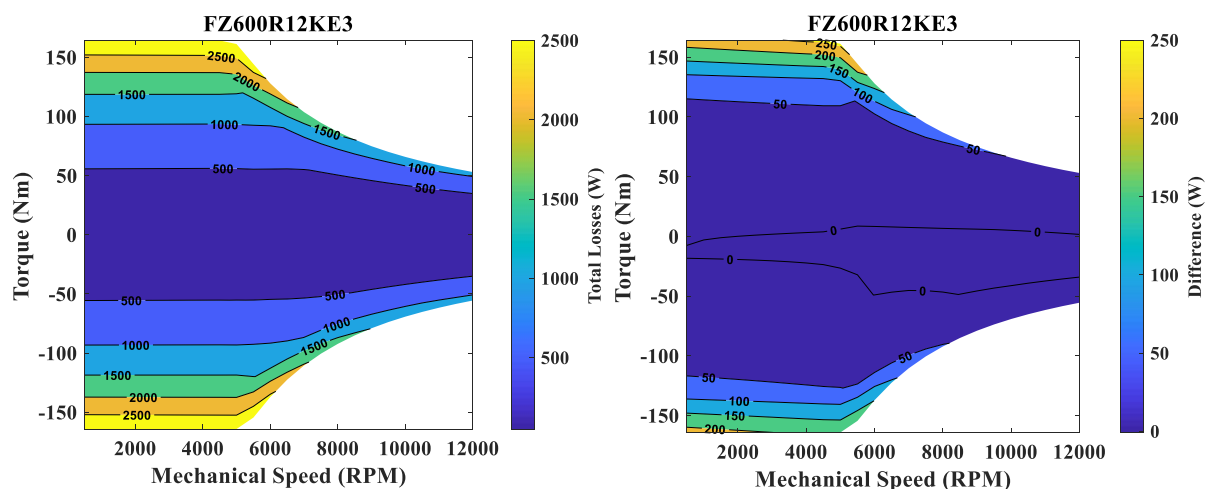


Fig. 6. Torque-speed map of the total losses with thermal feedback (left) and the loss difference between thermal and no thermal effect (right) in the FZ600 inverter.

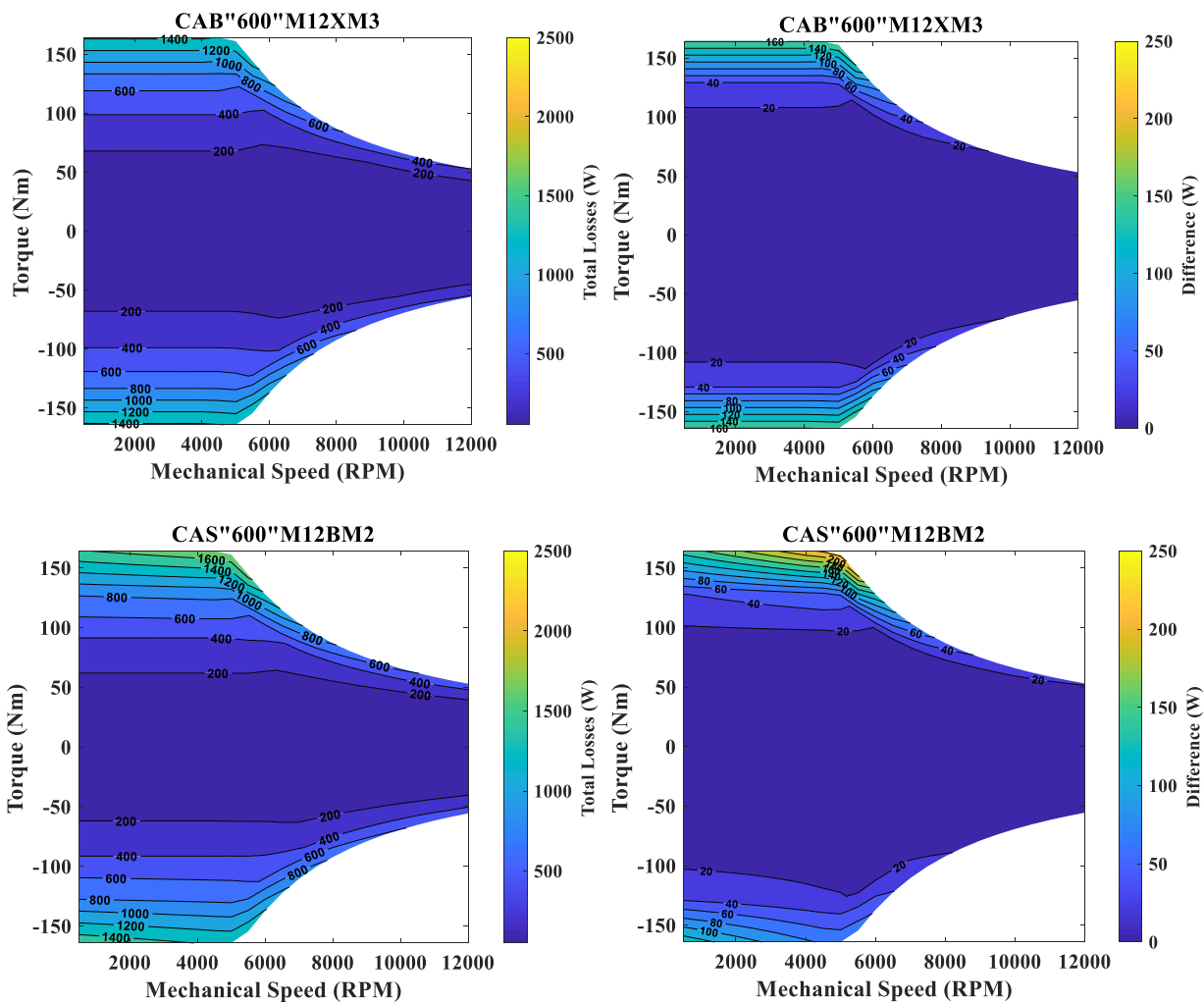


Fig. 7. Torque-speed map of the total losses with thermal feedback (left) and the loss difference between thermal and no thermal effect (right) in the CAB “600” (top) and CAS “600” (bottom) propulsion inverters.

all the operating points as well as when the blanking time and MOSFET’s reverse conduction are taken into account.

The effect of applying the thermal feedback on the losses are compared for the three inverters in the loss difference figures (right). A loss increase, up to 160 W and 220 W are observed for the CAB“600” and CAS“600” inverters, respectively, as well as up to 260 W loss increase for the FZ600 inverter.

Moreover, as shown in Figs. 6 and 7, the two SiC inverters offer up to 50% lower total losses when compared to those of the Si IGBT inverter, due to lower switching losses of the SiC MOSFETs as well as lower total conduction losses.

VIII. INVERTER TOTAL POWER LOSS VS SWITCHING FREQUENCY

The influence of different switching frequencies on the total losses for SiC MOSFET and IGBT inverters are presented in Fig. 8. From the figure, in the switching frequency range up to 2-3 kHz, all three modules show comparable power losses, but with the switching frequency increase, the strength of using the SiC MOSFETs is obvious. This is the consequence of higher switching energies of Si-IGBT modules along with their high temperature dependency when compared to those of the SiC MOSFET modules.

IX. CONCLUSION

This paper presents an investigation of the power losses, comparing a Si IGBT and two SiC inverters while considering as well as neglecting the effect of the thermal feedback. The effect is applied on a chosen operating point of a PMSM at high torque, low speed as well as for the all operating regions. For the Si IGBTs, the total switching loss increment with respect to temperature is more rapid

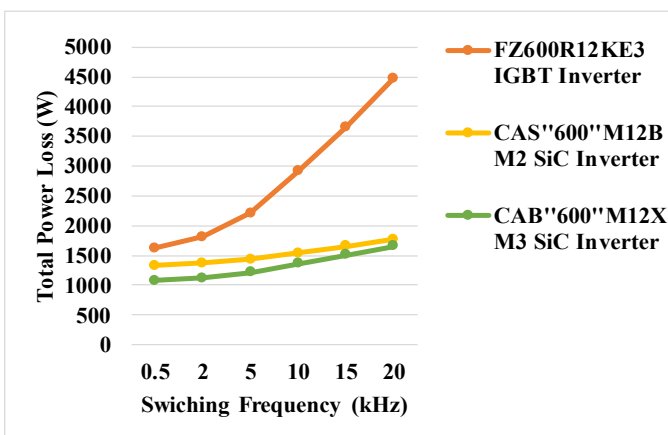


Fig. 8. Total power losses of IGBT and SiC MOSFETs’ inverters at different switching frequencies.

compared to the conduction loss. In SiC MOSFETs the conduction losses are increasing more rapidly with the junction temperature increase. The Si IGBTs are better in terms of conduction losses while the SiC MOSFETs have significantly lower switching power losses. Thus, Si IGBTs are a better solution at lower switching frequency while the SiC MOSFETs are superior at higher switching frequencies, as well as at high torque and low speed, using the benefit of their reverse conduction.

ACKNOWLEDGMENT

The financial support given by the national energy administration, Energimyndigheten, as well as CEVT is gratefully acknowledged.

REFERENCES

- [1] J. Reimers, L. Dorn-Gomba, Ch. Mak, A. Emadi, "Automotive Traction Inverters: Current Status and Future Trends," IEEE Transactions on Vehicular Technology, February 2019.
- [2] K. Kumar, M. Bertoluzzo and G. Buja, "Impact of SiC MOSFET traction inverters on compact-class electric car range," IEEE PEDES 2014.
- [3] J. Biela, M. Schweizer, S. Waffler and J.W. Kolar, "SiC versus Si-Evaluation of Potentials for Performance Improvement of Inverter and DC-DC Converter Systems by SiC Power Semiconductors," IEEE Transactions on Industrial Electronics, vol. 58, , no 7, Clarendon, July 2011.
- [4] X. Ding, M. Du, T. Zhou, H. Guo, C. Zhang, and F. Chen, "Comprehensive comparison between sic-mosfets and si-igbts based electric vehicle traction systems under low speed and light load," Energy Procedia, vol. 88, pp. 991-997, 2016.
- [5] J. Rabkowski and T. Platek, "Comparison of the power losses in 1700V Si IGBT and SiC MOSFET modules including reverse conduction," EPE'15 ECCE-Europe.
- [6] A. Acquaviva and T. Thiringer, "Energy efficiency of a SiC MOSFET propulsion inverter accounting for the MOSFET's reverse conduction and the blanking time," EPE 2017 ECCE Europe.
- [7] J. W. Kolar, H. Ertl and F. C. Zach, "Influence of the modulation method on the conduction and switching losses of a PWM converter system," IEEE Transactions on Industry Applications, vol. 21, no 6, 1991, pp 1063-1075.
- [8] F. Casanellas, "Losses in PWM inverters using IGBTs," IEEE Proc.-Electr. Power Appl., vol.141, no 5, pp.235-239.
- [9] SEMIKRON, Application Manual Power Semiconductors, ISLE Verlag 2015, Ilmenau, ISBN 978-3-938843-83-3, pp. 274-279.
- [10] M. Meyer and J. Böcker, "Optimum Control for Interior Permanent Magnet Synchronous Motors (IPMSM) in Constant Torque and Flux Weakening Range," EPE-PEMC 2006, pp. 282-286.
- [11] M. Meyer, T. Grote and J. Böcker, "Direct Torque Control for Interior Permanent Magnet Synchronous Motors with Respect to Optimal Efficiency," EPE 2007.